JOURNAL OF GEOPHYSICAL RESEARCH, VOL. 105, NO. D9, PAGES 11,767–11,780, MAY 16, 2000

Remote sensing of cloud properties using MODIS airborne simulator imagery during SUCCESS
1. Data and models

Bryan A. Baum,[1] David P. Kratz,[1] Ping Yang,[2] S.C. Ou,[3] Yongxiang Hu,[4,5]
Peter F. Soulen,[6,7] and Si-Chee Tsay[7]

Abstract. We investigate methods to infer cloud properties such as cloud optical thickness, thermodynamic phase, cloud particle size, and cloud overlap by comparing cloud and clear-sky radiative transfer computations to measurements provided by the Moderate Resolution Imaging Spectroradiometer (MODIS) airborne simulator (MAS). The MAS scanning spectroradiometer was flown on the NASA ER-2 during the Subsonic Aircraft Contrail and Cloud Effects Special Study (SUCCESS) field campaign during April and May 1996. The MAS bands chosen for this study correspond to wavelengths of 0.65, 1.63, 1.90, 2.15, 3.82, 8.52, 11, and 12 μm. Clear-sky absorption due to water vapor, ozone, and other trace gases is calculated using a set of correlated *k*-distribution routines developed specifically for these MAS bands. Scattering properties (phase function, single-scattering albedo, and extinction cross section) are derived for water droplet clouds using Mie theory. Scattering properties for ice-phase clouds are incorporated for seven cirrus models: cirrostratus, cirrus uncinus, cold cirrus, warm cirrus, and cirrus at temperatures of T = -20°C, -40°C, and -60°C. The cirrus are composed of four crystal types: hexagonal plates, two-dimensional bullet rosettes, hollow columns, and aggregates. Results from comparison of MAS data from a liquid water cloud with theoretical calculations indicate that estimates of optical thickness and particle size are reasonably consistent with one another no matter which spectral bands are used in the analysis. However, comparison of MAS data from a cirrus cloud with theoretical calculations shows consistency in optical thickness but not with particle size among the various band combinations used in the analysis. The methods described in this paper are used in two companion papers to explore techniques to infer cloud thermodynamic phase and cloud overlap.

1. Introduction

The retrieval of global cloud properties depends on accurate interpretation of satellite radiometric data. Retrievals of cirrus cloud properties from satellite-measured radiances are especially difficult because of the wide range of cirrus heights, particle sizes [*Heymsfield and Platt*, 1984; *Heymsfield et al.*, 1990], particle shapes [*Arnott et al.*, 1994; *Lawson et al.*, 1998] and their scattering properties [e.g., *Takano and Liou*, 1989a, b; *Yang et al.*, 1997; *Yang and Liou*, 1998], and the resulting large spatial and temporal variability of cirrus emittances and optical thicknesses [e.g., *Platt and Dilley*, 1979; *Sassen et al.*, 1990; *Spinhirne and Hart*, 1990; *Wielicki and Parker*, 1992]. The task of deriving cirrus properties from satellite data becomes even more difficult when cirrus appears simultaneously with other cloud types. Because of the difficulty in analyzing scenes that contain cloud overlap, operational cloud retrieval algorithms such as the International Satellite Cloud Climatology Project (ISCCP) by necessity employ the simplifying assumption that each satellite field of view (FOV) contains a single cloud layer.

The ability to remotely sense cloud properties will be enhanced when the new generation of cloud imagers are launched, beginning with an Earth-viewing sensor called the Moderate-Resolution Imaging Spectroradiometer (MODIS) that has been developed as the primary imager for the Earth Observing System-Terra and PM platforms. MODIS will provide images in 36 spectral bands between 0.415 and 14.2 μm with spatial resolutions of 250 m (two visible bands), 500 m (five bands), and 1000 m (29 bands). To support MODIS algorithm development, an aircraft version of the imager called the MODIS airborne simulator (MAS) has been installed and operated on the NASA high-altitude ER-2 research aircraft for a number of field campaigns, including SUCCESS, over a wide range of environmental conditions and surfaces.

The Subsonic Aircraft Contrail and Cloud Effects Special Study (SUCCESS) project conducted a multiaircraft field campaign during April and May 1996, primarily in close proximity to the Department of Energy (DOE) Atmospheric Radiation Measurement (ARM) program cloud and radiation test bed (CART) site. Among the goals of the project [*Toon and Miake-Lye*, 1998] are the investigation of the effect of aircraft

[1]NASA Langley Research Center, Hampton, Virginia.
[2]Science Systems and Applications, Inc., Lanham, Maryland.
[3]Department of Atmospheric Sciences, University of California at Los Angeles.
[4]Hampton University, Hampton, Virginia.
[5]Now at NASA Langley Research Center, Hampton, Virginia.
[6]Joint Center for Earth Systems Technology, University of Maryland Baltimore County, Catonsville.
[7]NASA Goddard Space Flight Center, Greenbelt, Maryland.

This paper is not subject to U.S. copyright. Published in 2000 by the American Geophysical Union.

Paper number 1999JD901089.

exhaust and condensation trails (contrails) on the Earth's radiative energy balance, the formation of cirrus clouds, and heterogeneous atmospheric chemistry. This study focuses on the remote sensing of cloud properties, such as cloud thermodynamic phase, particle size, and optical thickness, in scenes containing both single-layered and multilayered clouds.

6.25 scans/s. Each scan line contains 716 Earth-viewing pixels with a maximum scan angle extending approximately 43° on either side of nadir. The spatial resolution is 50 m at nadir at a nominal ER-2 altitude of 20 km, as compared with the 250-1000 m (at nadir) resolution of the MODIS instrument on the EOS satellites. Beginning in 1995, the 8-bit data system was replaced

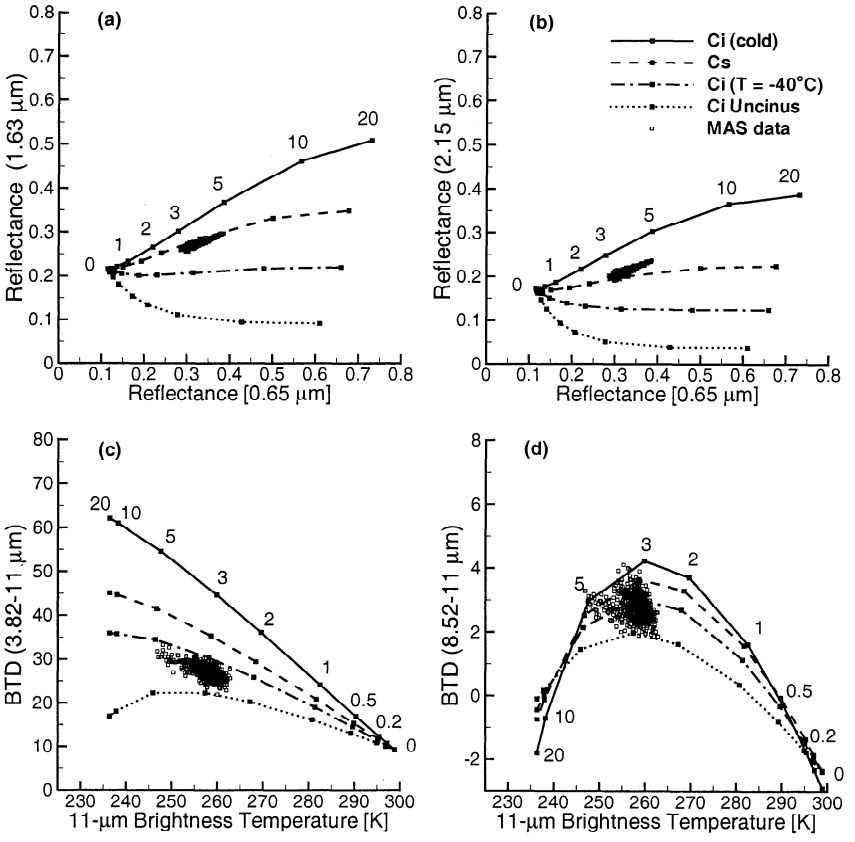

Figure 10. Comparison of theoretical results with MAS reflectance and BTD measurements recorded from a cirrus cloud on April 21, 1996, from region B (see Figure 8). Results are shown for (a) the reflectance at 1.63 μm versus the reflectance at 0.65 μm; (b) the reflectance at 2.15 μm versus the reflectance at 0.65 μm; (c) the BTD(3.82-11 μm) versus the 11-μm brightness temperature, and (d) the BTD(8.52-11 μm) versus the 11-μm brightness temperature. Visible (0.65 μm) optical thicknesses are provided in the curves.

3.82, 8.52, 11, and 12 μm), clear-sky absorption due to water vapor, ozone, and other trace gases is calculated using a set of correlated *k*-distribution routines developed specifically for this set of MAS bands. For each of the wavelengths listed above, scattering properties (phase function, single-scattering albedo, and extinction cross section) are utilized for both water droplet and ice-phase clouds. Scattering properties for ice phase clouds are incorporated for seven cirrus models. The cirrus are composed of four crystal types: hexagonal plates, two-dimensional bullet rosettes, hollow columns, and aggregates.

Results from comparison of MAS data from a liquid water cloud with theoretical results indicate that estimates of optical thickness and particle size are consistent with one another no matter which bands are used in the analysis.

The comparison of MAS data from a cirrus cloud with theoretical calculations show that the range of estimates of optical thickness are consistent among the various bands selected for comparison. Interestingly, the estimates of particle size are not consistent among the various band combinations. The main source of the uncertainty seems to be with the interpretation of the 3.82-μm MAS data, which is one of the most difficult to model due to the sensitivity of measured radiances at this wavelength to both reflected sunlight and thermal infrared emission. When we obtain a more extensive set of cirrus scattering properties we will perform a thorough sensitivity study to determine the sensitivity of the theoretical calculations to the assumed size distribution or to the assumed distribution of ice-crystal shapes.

Appendix

It is sometimes expedient to perform radiative transfer calculations with truncated phase functions; this is primarily due to the strong forward peaks of the actual phase functions at 0.65-, 1.63-, 1.90-, and 3.82-μm wavelengths. To achieve the same result in multiple-scattering computations with the truncated phase functions as with the nontruncated phase functions, an adjustment must be made to the optical thickness and single-scattering albedo. For both water- and ice-phase clouds, there is a strong contribution in the forward scattering direction due to diffraction. An additonal contribution to the strong forward peaks of the phase functions of polyhedral ice crystals is caused by δ transmission through parallel planes of the polyhedral crystals at a scattering angle of 0° [*Takano and Liou*, 1989a]. The fractions of scattered energy residing in the forward peak due to diffraction f and δ-transmission f_δ are removed from the scattering parameters using the similarity principle. Primes are used to denote the radiative parameters adjusted for diffraction. Double primes are used to denote the scattering parameters adjusted for both diffraction and δ transmission through opposing basal planes.

The extinction optical thickness (τ) is the sum of of the

scattering (τ_s) and absorption (τ_a) optical thicknesses. Since the strong diffraction forward peak has no contribution from absorption, the adjusted scattering and absorption optical thicknesses are

$$\tau'_s = (1-f)\tau_s, \tag{5}$$

$$\tau'_a = \tau_a. \tag{6}$$

The adjusted extinction optical thickness is then

$$\tau' = \tau'_s + \tau'_a = (1-f\tilde{\omega})\tau. \tag{7}$$

The adjusted single-scattering albedo may be expressed as

$$\tilde{\omega}' = \frac{\tau'_s}{\tau'} = \frac{(1-f)\tilde{\omega}}{1-f\tilde{\omega}}. \tag{8}$$

To adjust the scattering parameters for δ-transmission, a second adjustment is made similarly to that in equations (6) and (7), so the extinction optical thickness and single-scattering albedo become

$$\tau'' = (1-f_\delta\tilde{\omega})\tau, \tag{9}$$

$$\tilde{\omega}'' = \frac{(1-f_\delta)\tilde{\omega}}{1-f_\delta\tilde{\omega}}. \tag{10}$$

As *Takano and Liou* [1989a] point out, the expressions for optical thickness and single-scattering albedo scaled for both diffraction and δ transmission can be simplified to

$$\tau'' = (1-f''\tilde{\omega}')\tau', \tag{11}$$

$$\tilde{\omega}'' = \frac{(1-f'')\tilde{\omega}'}{1-f''\tilde{\omega}'}, \tag{12}$$

where

$$f'' = f + f_\delta - ff_\delta. \tag{13}$$

Again, there is no δ-transmission adjustment for water droplet clouds. Further, the δ transmission becomes very small at longer wavelengths because of increasing absorption.

Acknowledgments. Work on the derivation of ice-crystal scattering properties was supported by a MODIS contract to UCLA (contract NAG5-6160). The authors express their appreciation to the useful comments from two anonymous reviewers and from Chris Moeller and Andrew Heymsfield. The authors also thank Liam Gumley for providing the MAS imaging software.

References

Arnott, W. P., Y. Y. Dong, J. Hallett, and M. R. Poellot, Role of small ice crystals in radiative properties of cirrus: A case study, FIRE II, November 22, 1991, *J. Geophys. Res.*, *99*, 1371-1381, 1994.

Baum, B. A., and J. D. Spinhirne, Remote sensing of cloud properties using MODIS airborne simulator imagery during SUCCESS, 3, Cloud overlap, *J. Geophys. Res.*, this issue.

Baum, B. A., R. F. Arduini, B. A. Wielicki, P. Minnis, and S-C. Tsay, Multilevel cloud retrieval using multispectral HIRS and AVHRR data: Nighttime oceanic analysis, *J. Geophys. Res.*, *99*, 5499-5514, 1994.

Baum, B. A., P. F. Soulen, K. I. Strabala, M. D. King, S. A. Ackerman, W. P. Menzel, and P. Yang, Remote sensing of cloud properties using MODIS airborne simulator imagery during SUCCESS, 2, Cloud thermodynamic phase, *J. Geophys. Res.*, this issue.

Downing, H. D., and D. Williams, Optical constants of water in the infrared, *J. Geophys. Res.*, *80*, 1656-1661, 1975.

Gosse, S., D. Labrie, and P. Chylek, Refractive index of ice in the 1.4-7.8 μm spectral range, *Appl. Opt.*, *34*, 6582-6586, 1995.

Hansen, J. E., and L. D. Travis, Light scattering in planetary atmospheres, *Space Sci. Rev.*, *16*, 527-610, 1974.

Heymsfield, A. J., Cirrus uncinus generating cells and the evolution of cirroform clouds, part I, Aircraft observations of the growth of the ice phase, *J. Atmos. Sci.*, *32*, 799-808, 1975.

Heymsfield, A. J., and C. M. R. Platt, A parameterization of the particle size spectrum of ice clouds in terms of the ambient temperature and the ice water content, *J. Atmos. Sci.*, *41*, 846- 855, 1984.

Heymsfield, A. J., K. M. Miller, and J. D. Spinhirne, The 27-28 October 1986 FIRE IFO Cirrus Case Study: Cloud microstructure, *Mon. Weather Rev.*, *118*, 2313-2328, 1990.

King, M. D., et al., Airborne scanning spectrometer for remote sensing of cloud, aerosol, water vapor, and surface properties, *J. Atmos. Oceanic Technol.*, *13*, 777-794, 1996.

Kratz, D. P., The correlated *k*-distribution technique as applied to the AVHRR bands, *J. Quant. Spectrosc. Radiat. Transfer*, *53*, 501-517, 1995.

Kratz, D. P., and F. G. Rose, Accounting for molecular absorption within the spectral range of the CERES window band, *J. Quant. Spectrosc. Radiat. Transfer*, *61*, 83-95, 1999.

Kurucz, R. L., I. Furenlid, J. Brault, and L. Testerman, Solar flux atlas from 296 to 1300 nm, in *National Solar Observatory Atlas no. 1*, 239 pp., Nat. Solar Obs., Sunspot, N. M., 1984.

Lawson, R. P., A. J. Heymsfield, S. M. Aulenbach, and T. L. Jensen, Shapes, sizes, and light scattering properties of ice crystals in cirrus and a persistent contrail during SUCCESS, *Geophys. Res. Lett.*, *25*, 1331-1334, 1998.

Moeller, C. C., P. S. Grant, D. D. LaPorte, L. E. Gumley, P. Hajek, W. P. Menzel, J. S. Myers, and S. White, Blackbody emissivity considerations for radiometric calibration of the MODIS Airborne Simulator (MAS) thermal bands, *SPIE*, *2820*, 44-55, 1996.

Moeller, C. C., D. D. LaPorte, P. Hajek, K. I. Strabala, and W. P. Menzel, Spectral characterization of MODIS Airborne Simulator (MAS) LWIR bands and application to MODIS science data cloud products, *SPIE*, *3117*, 235-243, 1997.

Neckel, H., and D. Labs, The solar radiation between 3300 and 12500 angstroms, *Sol. Phys.*, *90*, 205-258, 1984.

Platt, C.M.R, and A. C. Dilley, Remote sounding of high clouds, II, Infrared emissivity of cirrostratus, *J. Appl. Meteorol.*, *18*, 1144-1150, 1979.

Press, W. H., B. P. Flannery, S. A. Teukolsky, and W. T. Vetterling, *Numerical Recipes*, 839 pp., Cambridge Univ. Press, New York, 1986.

Sassen, K., C. J. Grund, J. Spinhirne, M. Hardesty, and J. M. Alvarez, The 27-28 October 1986 FIRE IFO cirrus case study: A five lidar overview of cloud structure and evolution, *Mon. Weather Rev.*, *118*, 2288-2311, 1990.

Smith, W. L., et al., Observations of the infrared radiative properties of the ocean—Implications for the measurement of sea surface temperature via satellite remote sensing, *Bull. Am. Meteorol., Soc.*, *77*, 41-51, 1996.

Spinhirne, J. D., and W. D. Hart, Cirrus structure and radiative parameters from airborne lidar and spectral radiometer observations: The 28 October case study, *Mon. Weather Rev.*, *118*, 2329-2343, 1990.

Stone, R. S., G. L. Stephens, C. M. R. Platt, and S. Banks, The remote sensing of thin cirrus cloud using satellites, lidar and radiative transfer theory, *J. Appl. Meteorol.*, *29*, 353-366, 1990.

Takano, Y., and K.-N. Liou, Solar radiative transfer in cirrus clouds, part 1, Single-scattering and optical properties of hexagonal ice crystals, *J. Atmos. Sci.*, *46*, 3-19, 1989a.

Takano, Y., and K.-N. Liou, Solar radiative transfer in cirrus clouds, part 2, Theory and computation of multiple scattering in an anisotropic medium, *J. Atmos. Sci.*, *46*, 20-36, 1989b.

Toon, O. B., and R. C. Miake-Lye, Subsonic aircraft: Contrail and cloud effects special study (SUCCESS), *Geophys. Res. Lett.*, *25*, 1109-1112, 1998.

Tsay, S.-C., K. Stamnes, and K. Jayaweera, Radiative transfer in stratified atmospheres: Development and verification of a unified model, *J. Quant. Spectrosc. Radiat.Transfer*, *43*, 133- 148, 1990.

Warren, S. G., Optical constants of ice from the ultraviolet to the microwave, *Appl. Opt.*, *23*, 1206-1225, 1984.

Wielicki, B. A., and L. Parker, On the determination of cloud cover from satellite sensors: The effect of sensor spatial resolution, *J. Geophys. Res.*, *97*, 12,799-12,823, 1992.

Wiscombe, W. J., Improved Mie scattering algorithm, *Appl. Opt.*, *19*, 1505-1507, 1980.

Wyser, K., and P. Yang, Average ice crystal size and bulk shortwave single scattering properties for cirrus clouds, *Atmos. Res.*, *49*, 315-335, 1998.

Yang, P., and K.N. Liou, Finite-difference time domain method for light scattering by small ice crystals in three-dimensional space, *J. Opt. Soc. Am. A.*, *13*, 2072-2085,1996a.

Yang, P., and K.N. Liou, Geometric-optics-integral-equation method for light scattering by nonspherical ice crystals, *Appl. Opt.*, *35*, 6568-6584, 1996b.

Yang, P., and K. N. Liou, Single-scattering properties of complex ice crystals in terrestrial atmosphere, *Contrib. Atmos. Phys.*, *71*, 223-248, 1998.

Yang, P., K.N. Liou, and W. P. Arnott, Extinction efficiency and single-scattering albedo for laboratory and natural cirrus clouds, *J. Geophys. Res.*, *102*, 21,825-21,835, 1997.

B. A. Baum, NASA/CIMS, 1225 West Dayton St., Madison, WI 53706. (bryan.baum@ssec.wisc.edu).

Y. Hu, NASA Langley Research Center, Hampton, VA 23681-2199.

D. P. Kratz, NASA Langley Research Center, Hampton, VA 23681-2199.

S. C. Ou, Department of Atmospheric Sciences, University of California at Los Angeles, CA 90032.

P. F. Soulen, Joint Center for Earth Systems Technology, University of Maryland, Baltimore County, Catonsville, MD 21228.

S.-C. Tsay, NASA Goddard Space Flight Center, Greenbelt, MD 20771.

(Received May 21, 1999; revised October 6, 1999; accepted October 13, 1999.)